MDPI

Article

Microgrid Energy Management System for Residential Microgrid Using an Ensemble Forecasting Strategy and Grey Wolf Optimization

Usman Bashir Tayab [1,2,]*[iD], Junwei Lu [1], Seyedfoad Taghizadeh [3][iD], Ahmed Sayed M. Metwally [4][iD] and Muhammad Kashif [5][iD]

1   School of Engineering and Built Environment, Griffith University, Gold Coast, QLD 4215, Australia; j.lu@griffith.edu.au
2   Department of Electrical and Biomedical Engineering, RMIT University, Melbourne, VIC 3001, Australia
3   School of Engineering, Macquarie University, Macquarie Park, NSW 2019, Australia; s.t.taghizadeh@ieee.org
4   Department of Mathematics, College of Science, King Saud University, Riyadh 11451, Saudi Arabia; dalsayed@ksu.edu.sa
5   School of Electrical and Information Engineering, Tianjin University, Tianjin 300072, China; mkashif@tju.edu.cn
*   Correspondence: usmanbashir.tayab@griffithuni.edu.au or usman.bashir.tayab@rmit.edu.au or usman.tayab@yahoo.com

check for updates

Abstract: Microgrid (MG) is a small-scale grid that consists of multiple distributed energy resources and load demand. The microgrid energy management system (M-EMS) is the decision-making centre of the MG. An M-EMS is composed of four modules which are known as forecasting, scheduling, data acquisition, and human-machine interface. However, the forecasting and scheduling modules are considered the major modules from among the four of them. Therefore, this paper proposed an advanced microgrid energy management system (M-EMS) for grid-connected residential microgrid (MG) based on an ensemble forecasting strategy and grey wolf optimization (GWO) based scheduling strategy. In the forecasting module of M-EMS, the ensemble forecasting strategy is proposed to perform the short-term forecasting of PV power and load demand. The GWO based scheduling strategy has been proposed in scheduling module of M-EMS to minimize the operating cost of grid-connected residential MG. A small-scale experiment is conducted using Raspberry Pi 3 B+ via the python programming language to validate the effectiveness of the proposed M-EMS and real-time historical data of PV power, load demand, and weather is adopted as inputs. The performance of the proposed forecasting strategy is compared with ensemble forecasting strategy-1, particle swarm optimization based artificial neural network, and back-propagation neural network. The experimental results highlight that the proposed forecasting strategy outperforms the other strategies and achieved the lowest average value of normalized root mean square error of day-ahead prediction of PV power and load demand for the chosen day. Similarly, the performance of GWO based scheduling strategy of M-EMS is analyzed and compared for three different scenarios. Finally, the experimental results prove the outstanding performance of the proposed scheduling strategy.

Keywords: energy management system; grey wolf optimization; forecasting; microgrid; particle swarm optimization

1. Introduction

The control and management of microgrid (MG) are responsible for handling several issues such as frequency and voltage regulation, the intermittent nature of renewable energy resources (RES), the mismatch among generation and load demand, and battery energy storage systems (BESS) [1]. Adopting the hierarchical control approach as a structured solution in MG is prompted by the diversity of control aspects, particularly when several processes are needed to complete multiple tasks [2,3]. Generally, the hierarchical control

of MG is segregated into three levels, i.e., primary, secondary, and tertiary level. The primary level of control performs the local control of MG, which includes power sharing and voltage and frequency regulation, while the secondary level performs the restoration of voltage and frequency along with the synchronization. Finally, the tertiary level, which is known as the MG energy management system (M-EMS), manages the power flow among different available power generation resources to meet the load demand. The scope of this research work is focused on the final level of hierarchical control of MG. When several RES and BESS are available in MG as energy resources, then M-EMS is essential to meet the desired objectives of MG [4]. The MG-EMS provides a sequence of reference commands that determine the operation of each available power source and guide the power flow within the MG. The requirement of M-EMS is necessary for both modes of operation of MG. However, the role of M-EMS depends on the configuration of MG. For example, the M-EMS controls the power flow from and to the main grid during the grid-connected mode of operation [5].

Over the past few years, researchers have proposed several M-EMSs for grid-connected MG. A rule-based EMS has been proposed in a previous study [6], for grid-connected MG and simulated using the PSCAD software. The proposed model ensures the economical and reliable operation of the PV, battery, and fuel cell-based grid-connected MG. The master/slave control is also used to maintain the voltage and frequency stability of the MG system. The concept of prosumers in the grid-connected MG system was introduced in [7]. The MG system is composed of prosumers and a microturbine. A prosumer consists of a PV, a BESS, and an ultra-capacitor. The proposed EMS contains two parts, namely, the central EMS and the local power management system. Rule-based central EMS controls power flow within an MG to meet prosumer demand, and reference power is provided in the EMS to maintain the prepared power-sharing among different power generation units with an interval of 0.5 h. By contrast, the local power management system maintains the primary frequency regulation and power balance within an MG.

To minimize the operating costs of grid-connected MG, Fossati et al. [8] proposed a novel energy management system (EMS) that applies two genetic algorithm (GA)-based fuzzy logic controllers. The first GA is used to schedule power with an MG and set the fuzzy rule of the expert system, whereas the second GA optimally tunes the membership functions of the fuzzy logic controller. The effectiveness of the proposed method is determined by comparing its performance with the simple rule- and manually tuned fuzzy logic controller-based EMSs. Similarly, for a grid-connected MG, Santis et al. [9] proposed a fuzzy expert system-based EMS that performs better than the classic GA-based model. The hierarchical GA is used to tune the minimum rule-based fuzzy logic controller of EMS, and the efficiency parameters of BESS improve the MG performance.

A mixed-mode EMS was previously proposed [10] for grid-connected MG, implemented for three different operational modes, namely, on/off, power-sharing and continuous run modes. The solutions use mixed-integer linear programming (MILP) for the on/off mode and LP for the latter two. BESS sizing is also computed to meet the operational requirements of MG. An optimal EMS was previously proposed [11] to minimize the operating costs of residential MG, including energy cost, penalty cost on adjustable load, associated cost and range anxiety term of the EV battery. The critical, adjustable and movable loads were considered, and the range anxiety term EV battery was taken as the fear factor of energy drain before reaching the target location. The designed MG system was managed using MILP to achieve the desired objectives.

Shen et al. introduced a MILP-based EMS for peak shaving application to maximize revenue by using renewable resources and BESS-based MG [12]. The authors considered the demand response scheme and assumed that the load demand of MG is always higher than that of the power generation. Two new indices related to peak shaving are introduced by the author. One bus and an IEEE 14 bus MG system are also simulated to validate the effectiveness of the proposed model. Similarly, a MILP-based EMS was implemented to minimize the operating and maintenance costs of the MG system, along with the demand

response scheme and three different types of loads, namely, curtailable, reschedulable and critical load demand [13]. The proposed concept was verified through MATLAB, and the simulation results indicated the advantages of the proposed model.

A regrouping particle swarm optimization (PSO)-based scheduling method for industrial MG was presented in the previous studies [14,15]. The proposed scheduling strategy performed the 24-h-ahead optimum scheduling of the power generation units to feed the load demand. The objective function of the developed scheduling method includes the operating, maintenance, and purchasing power costs from the main grid. The proposed strategy provides better results than GA with respect to global optimum solution and computation time. Similarly, Faridnia et al. proposed a PSO-based scheduling method for MG that minimized the operational cost of tidal generation and BESS-based MG [16]. Alavi et al. proposed a PSO-based scheduling approach to perform the optimal operation of grid-connected MG [17]. The proposed framework minimized the operation, emission, and reliability cost of the MG. A point estimation approach on the basis of beta and Weibull density functions was used to model uncertainties of solar and wind power. Previous research [18] proposed a two-stage optimal energy and reserve management system using stochastic weight PSO for grid-connected MG. The proposed model performed power scheduling and estimated the reserve in the first stage. The second stage, reserve dispatch, was performed to handle the stochastic nature of renewable resources. The aim of the presented framework is to minimize load shedding, fuel consumption, emission, voltage deviation, and energy trade costs involved in MG utilization.

A hybrid differential evolution (DE) and modified PSO-based scheduling methods were proposed in the previous study to minimize the operational and emission cost of MG [19]. The proposed approach also considered demand response, time-of-use tariffs, and generation reserve schedule. In the previous studies, PSO and regularized PSO-based optimum scheduling methods were presented to perform the economic operation of MG [20–23]. The proposed method considers the stochastic nature of PV and wind power, as well as load demand and electricity price. The proposed model was simulated using MATLAB to verify the efficiency of the proposed approach compared with existing approaches. A previous research work introduced a GA-based scheduling approach to optimize power generation and for the reserve scheduling of grid-connected MG [24]. The scenario generation and reduction approach were used to model uncertainties of wind power and load. The objective function considers the operating, capital, active power reserve, purchasing power (from the grid), and reactive power support costs. Automatic controller status switches were used to improve the economic advantages of MG. Similarly, another scheduling method using GA was proposed in [25] that minimizes network losses, operational and emission costs of MG. The superior performance of the GA-based scheduling method was analyzed using simulation and compared with the MILP-based scheduling method.

Based on existing literature, it can be summarized that the forecasting and scheduling strategies in existing M-EMS can be further improved for effective and economical operation of MG. Therefore, this research work proposes an efficient M-EMS using ensemble forecasting strategy and grey wolf optimization-based scheduling strategy for grid-connected MG. The proposed strategy has been compared with several existing competitive strategies to prove the efficiency of proposed method. The main contributions of this research work are listed as follows:

- This paper proposed an ensemble forecasting strategy in the forecasting module of M-EMS for day-ahead prediction of PV power and load demand.
- The proposed forecasting strategy is compared with ensemble strategy-1, particle swarm optimization based artificial neural network (PSO-ANN), and back-propagation neural network (BPNN) to prove the effectiveness of the proposed ensemble forecasting strategy.
- A grey wolf optimization (GWO) based scheduling strategy is proposed in scheduling module of M-EMS to perform the optimum scheduling of available power resources

in grid-connected MG and analyzed the performance of proposed scheduling strategy for three different scenarios.

The rest of the paper is organized as follows. Section 2 provides a detailed description of the architecture of the understudy MG. A detailed description of the proposed forecasting and scheduling strategy of M-EMS is provided in Section 3. Section 4 presents the experimental results of the forecasting and scheduling strategy of M-EMS, while the conclusion is provided in Section 5.

2. System Description and Modeling

In this study, the performance of the proposed M-EMS is tested on a small-scale grid-connected residential MG using real time data of PV power and load demand. Figure 1 illustrates the structure of the understudy MG. The grid-connected residential MG is comprised of PV panels with a capacity of 7 kW and BESS with a capacity of 10 kWh. The residential MG has the ability to share the power with the main grid with a limit of 2.5 kW.
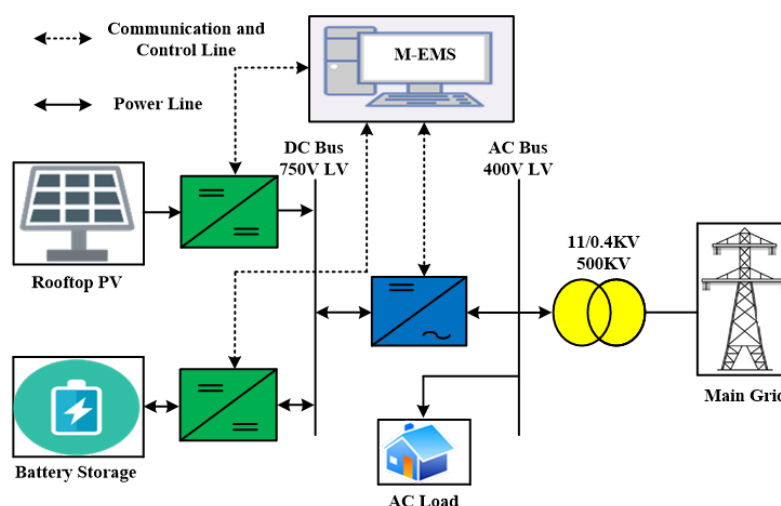

Figure 1. Structure of the understudy MG.

The M-EMS is mainly responsible for ensuring the stable and economical operation of the MG. The operating cost of the MG is minimized by proper utilization of BESS. The mathematical modeling of the PV and BESS is provided as follows:

- Photovoltaic Power Generation System: Photovoltaic (PV) generates electric power from solar energy via a PV module. The output power of the PV module depends on solar irradiation, atmospheric temperature, efficiency, and area of the PV module. The hourly output power of the PV system can be calculated using Equation (1).

$$P_{PV}(t) = A_{PV}n_{PV}R(t)[1 - 0.005(T(t) - 25)] \quad \forall t > 0 \tag{1}$$

where, A_{PV} is the area of the PV module in m^2, n_{PV} is the efficiency of the module, R is the solar irradiation in Wm^{-2} and T is atmospheric temperature in degrees centigrade.

- Battery Energy Storage System: A BESS is composed of series-parallel strings of batteries. There are several types of batteries available in the market which have different chemical characteristics, numbers of cycles, and depth of discharge. In this research, a lithium acid battery is used as a BESS. Lithium acid batteries have commonly been used for electric energy storage in residential MGs. The state of charge and discharge of BESS at each time interval can be calculated by following these mathematical equations:

In charge mode $(P_{BESS}(t) < 0)$

$$E_{BESS}(t) = E_{BESS}(t - 1) - \eta_{BC}P_{BC}(t)\Delta t \tag{2}$$

In discharge mode $(P_{BESS}(t) > 0)$

$$E_{BESS}(t) = E_{BESS}(t - 1) - \frac{P_{BD}(t)}{\eta_{BD}} \Delta t \qquad (3)$$

where $P_{BC}(t)$ and $P_{BD}(t)$ are the charging and discharging battery power (kW), $E_{BESS}(t)$ is battery energy (kWh), η_{BC} is battery charging efficiency, η_{BD} is battery discharge efficiency, Δt is the scheduling time step.

3. Proposed Microgrid Energy Management System

Figure 2 shows an intelligent M-EMS based on an improved hybrid forecasting and optimal scheduling proposed for grid-connected MG. The proposed M-EMS can be divided into several stages, as follows: collecting the weather, PV power, and load demand data; processing the input from historical data and forecasting the PV power and load demand; and optimally scheduling energy resources to meet the desired objective and load demand. Finally, the data acquisition (DAQ) and human–machine interface (HMI) modules allow users to analyze and monitor different input parameters, including historical weather, PV power and load demand data. Sections 3.1 and 3.2 provide a detailed description of the forecasting and scheduling modules of the M-EMS, respectively.
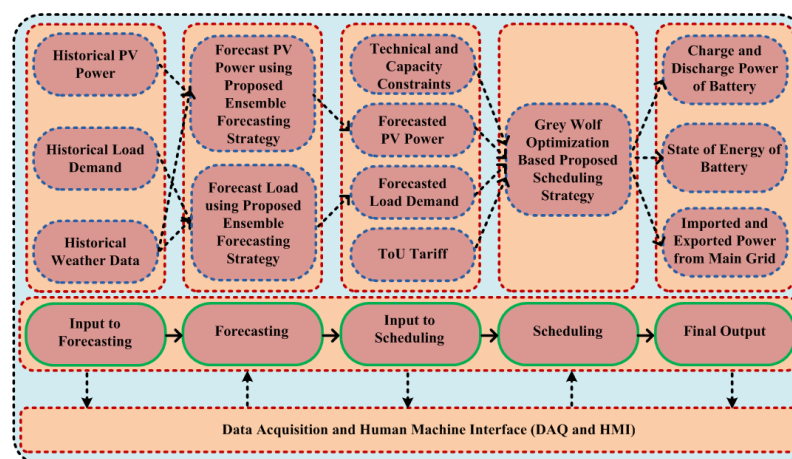

Figure 2. Proposed microgrid energy management system.

3.1. Proposed Forecasting Strategy

The proposed ensemble forecasting strategy is based on the systematic combination of three FNN models for day-ahead forecasting of PV power and load demand. These FNN models are trained by improved PSO to optimally calculate the weights and biases for improving forecasting accuracy. The output of all models is aggregated using the Bayesian model averaging (BMA) method, which can be seen in Figure 3. To perform the forecasting of PV power and load demand, the historical data of weather, PV power, and load demand are used as inputs for each model, and the details of historical data is mentioned in Section 4. After that, the outputs of all models are combined using the BMA method to gain the day-ahead forecasted values of PV power and load demand. The working process of the proposed ensemble strategy has several steps, which are described as follows:
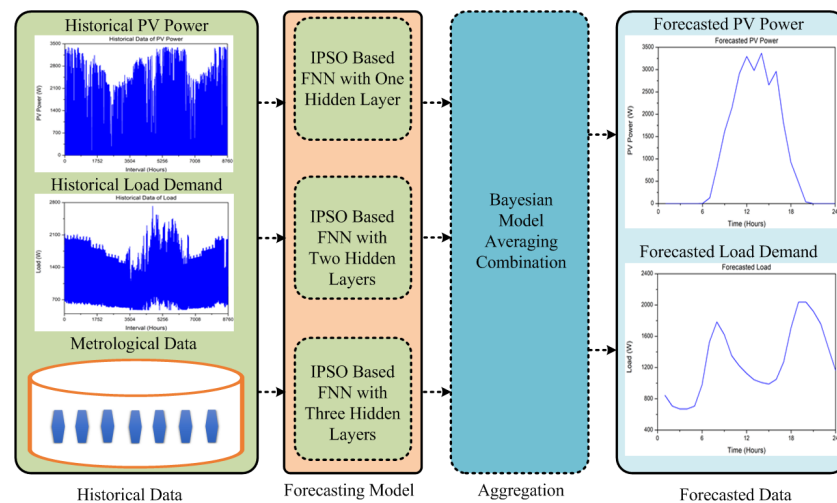
Figure 3. Proposed forecasting strategy.

1. Working Process of Proposed Strategy
    - Data Preprocessing: The input parameters of all forecasting models are selected based on correlation parameters with PV power and load demand for the forecasting of PV power and load demand. The selected parameters for PV power forecasting are historical data of PV power, solar irradiance, temperature, wind speed, and humidity. On the other hand, the chosen correlated parameters for load demand forecasting are the same parameters as the authors of [26] chose for load demand forecasting.
    - Construction of Forecasting Models in Ensemble Strategy: Figure 3 highlights the selected models in the proposed strategy. There are three FNN structures, i.e., FNN with one hidden layer, FNN with two hidden layers, and FNN with three hidden layers, that have been used in the proposed ensemble strategy. The details about the FNN structure can be found in [26]. The improved PSO is used to train each forecasting model, and the detail of the improved PSO is described in the following subsection.
    - Aggregation: The output of all forecasting models is aggregated using the BMA method for attaining highly accurate forecasting results. The BMA is a statistical method that combines the output of multiple forecasting models by inferring consensus between them. Based on the posterior probabilities of each model, the BMA approach assigns weights to individual forecasting models. In contrast to a less accurate model, the higher value of weights is assigned to the extremely accurate model. Further details about the BMA method can be seen in [27].

2. Improved Particle Swarm Optimization
   PSO is a population-based algorithm that was proposed by Kennedy and Eberhart in 1995 and inspired by offensive particle movement [28]. When the particles want to move, they use present position and neighbor particle positions in order to reach the particle with the best position. The particles are described with two vectors, i.e., particle velocity V_j and particle position x_i. In every movement step of the particle population, every particle is updated by two values. The first value is the best previous position of particle *i* that is called pbest and evaluated by using fitness function. The second value is the best particle among all p-bests and is called gbest. Any of the particles can update their new velocity and position by following equations:

$$V_j^{i+1} = w \cdot V_j^i + C_1 r_1 \cdot [P_{best} - x_j^i] + C_2 r_2 \cdot [G_{best} - x_j^i] \qquad j = 1, 2, 3......, n \qquad (4)$$

$$x_j^{i+1} = x_j^i + V_j^{i+1} \tag{5}$$

where r_1 and r_2 are random numbers that are selected in the interval of [0 1], w is the inertia weight which is calculated using Equation (6).

$$w = w_{max} - (w_{max} - w_{min}) \times \sqrt{\frac{t}{max\ iter}} \tag{6}$$

here, t is the current iteration, and *max iter* is the maximum number of iterations. The C_1 and C_2 are cognitive constants which are selected as constant in standard PSO. However, the author of [29] proposed mathematical equations to calculate the values of C_1 and C_2, which improved the performance of PSO. The values of C_1 and C_2 can be calculated as follows:

$$C_1 = \sqrt[2]{1 - \sin(\frac{\text{ß}}{2} \times \frac{t}{max\ iter})} \tag{7}$$

$$C_2 = \sqrt[2]{\sin(\frac{\text{ß}}{2} \times \frac{t}{max\ iter})} \tag{8}$$

3.2. Proposed Scheduling Strategy

A key component of EMS is the scheduling module, which optimally controls power flow in MGs to meet the objective function by setting decision variables. In this study, the objective of optimal power flow is to maximize the utilization of PV power and minimize the operational costs of MG. The objective function for each interval with respect to time can be defined as:

$$J = min \sum_{t=1}^{T} P_{PV}(t)C_{PV} + P_{BC}(t)C_{BESS} + P_{BD}(t)C_{BESS} + P_{G-I}(t)C_{G-I} - P_{G-E}(t)C_{G-E} \tag{9}$$

where C_{PV} and C_{BESS} are the operational and maintenance costs of PV and BESS, respectively; C_{G-I} and C_{G-E} are the costs of purchasing and selling power from the main grid at time interval t, respectively; and T is the total time for optimum scheduling, which is 24 h. The main decision variables for the grid-connected MG under study are the PV power (P_{PV}) imported and exported power (P_{G-I}, P_{G-E}) from/to the main grid, charge and discharge power (P_{BC}, P_{BD}) of BESS, binary decision variables (α, β) of BESS and the main grid and capacity of BESS (E_{BESS}). These decision variables are essential to achieve the economic operation of grid-connected MG. Note that in Equations (9) and (10), the values of P_{BC}, P_{G-E} are taken as absolute. In solving the optimal power flow problem, several systems require constraints and limitations. One such constraint is the system power balance as described by Equation (10).

$$P_{Load}(t) - P_{PV} - P_{BD}(t) - P_{G-I}(t) + P_{BC}(t) + P_{G-E}(t) = 0 \longrightarrow t\epsilon[1:T] \tag{10}$$

$$E_{BESS}(t) = E_{BESS}(t-1) - \eta_{BC}P_{BC}(t)\Delta t - \frac{P_{BD}(t)}{\eta_{BD}}\Delta t \longrightarrow t\epsilon[1:T] \tag{11}$$

$$P_{BC}(t) - P_{BC}^{max}\alpha \leqslant 0 \longrightarrow t\epsilon[1:T] \tag{12}$$

$$P_{BD}(t) + P_{BD}^{max}\alpha \leqslant P_{BD}^{max} \longrightarrow t\epsilon[1:T] \tag{13}$$

$$P_{G-E}(t) - P_{G-E}^{max}\beta \leqslant 0 \longrightarrow t\epsilon[1:T] \tag{14}$$

$$P_{G-I}(t) + P_{G-I}^{max}\beta \leqslant P_{G-I}^{max} \longrightarrow t\epsilon[1:T] \tag{15}$$

Other variables that need consideration in solving the optimization problem are upper and lower bounds which are listed below.

$$P_{PV}^{min} \leqslant P_{PV}(t) \leqslant P_{PV}^{max} \longrightarrow t\epsilon[1:T] \tag{16}$$

$$0 \leqslant P_{BC}(t) \leqslant P_{BC}^{max} \longrightarrow t\epsilon[1:T] \tag{17}$$

$$0 \leqslant P_{BD}(t) \leqslant P_{BD}^{max} \longrightarrow t\epsilon[1:T] \tag{18}$$

$$0 \leqslant P_{G-I}(t) \leqslant P_{G-I}^{max} \longrightarrow t\epsilon[1:T] \tag{19}$$

$$0 \leqslant P_{G-E}(t) \leqslant P_{G-E}^{max} \longrightarrow t\epsilon[1:T] \tag{20}$$

$$E_{BESS}^{min} \leqslant E_{BESS}(t) \leqslant E_{BESS}^{max} \longrightarrow t\epsilon[1:T] \tag{21}$$

$$E_{BESS}(0) = E_{BESS-initial} \tag{22}$$

$$E_{BESS-initial} = E_{BESS-end} \tag{23}$$

In this study, the grey wolf optimization (GWO) is applied to achieve optimum scheduling in a grid-connected residential MG. Mirjalili et al. (2014) proposed GWO as a swarm-based heuristic approach inspired by the social hierarchy and natural hunting behaviour of grey wolves [30]. Figure 4 shows that the social hierarchy of wolves can be divided into four categories. The first and top level, alpha, is composed of males and females that are responsible for decision-making, including hunting, sleep location and wake-up time. The second level is beta, which helps the alpha in decision making and implementing strategies at a lower level. Delta is the third level and tasked to follow instructions from above and control the omega, which is the lowest level in the hierarchy, follows commands of all groups and hunts for the pack.
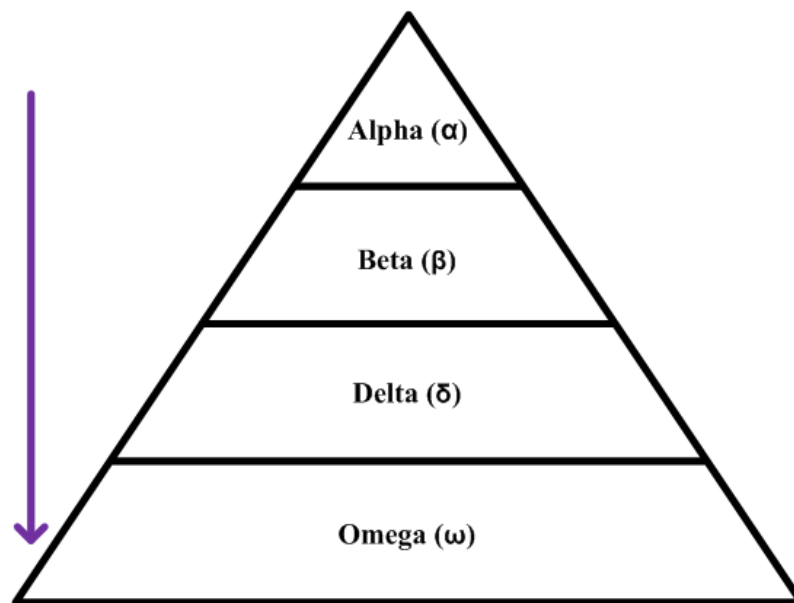

Figure 4. Hierarchy of the grey wolf.

In GWO, the first three best solutions are assumed as alpha, beta and delta while the remaining ones in the search space are considered as omega. While hunting, grey wolves surround the prey, a behaviour that can be described mathematically by Equations (24) and (25):

$$F = |G \cdot X_{prey}(t) - X(t)| \tag{24}$$

$$X(t+1) = X_{prey}(t) - D \cdot F \tag{25}$$

here, X_{prey} is the position of a prey, X is the position of a grey wolf, t is the present iteration, and D and G are coefficients as obtained by using Equations (26) and (27).

$$D = 2a \cdot r_1 - a \tag{26}$$

$$G = 2 \cdot r_2 \tag{27}$$

hence, r_1 and r_2 are random numbers between 0–1 while component a linearly decreases from 2 to 0 over the number of iterations. During the optimization, the best solutions of the first three parameters are saved and then used to update the position of the other wolves (omega). This update is represented in mathematical form by the following equations:

$$F_\alpha = |G_1 \cdot X_\alpha(t) - X(t)| \tag{28}$$

$$F_\beta = |G_2 \cdot X_\beta(t) - X(t)| \tag{29}$$

$$F_\delta = |G_3 \cdot X_\delta(t) - X(t)| \tag{30}$$

Based on the positions of the alpha, beta and delta, that of the prey is determined using the following equations:

$$X_1 = |X_\alpha - D_1 \cdot F_\alpha| \tag{31}$$

$$X_2 = |X_\beta - D_2 \cdot F_\beta| \tag{32}$$

$$X_3 = |X_\delta - D_3 \cdot F_\delta| \tag{33}$$

$$X(t+1) = \frac{X_1 + X_2 + X_3}{3} \tag{34}$$

where, X_α, X_β, and X_δ indicate the positions of the alpha, beta and delta, respectively. The exploration and exploitation of grey wolf search agents depend on the parameter D. Specifically, exploration occurs if $D \geqslant 1$ and exploitation occurs if $D < 1$.

4. Experimental Results and Discussion

In this section, the experimental results of the proposed M-EMS for small-scale residential MG are presented and Figure 5 shows small-scale experiment setup of residential MG. The proposed M-EMS is implemented using Raspberry Pi 3 B+ via python programming language, and the output pins of Raspberry Pi 3 B+ are digital. Therefore, an Adafruit MCP 4728 digital to analog converter is used to convert the digital output of Raspberry Pi 3 B+ into analog form to display the output on the oscilloscope and also sending the signal to the primary controller. Moreover, the local storage of Raspberry Pi 3 B+ is utilized for the purpose of data storage.
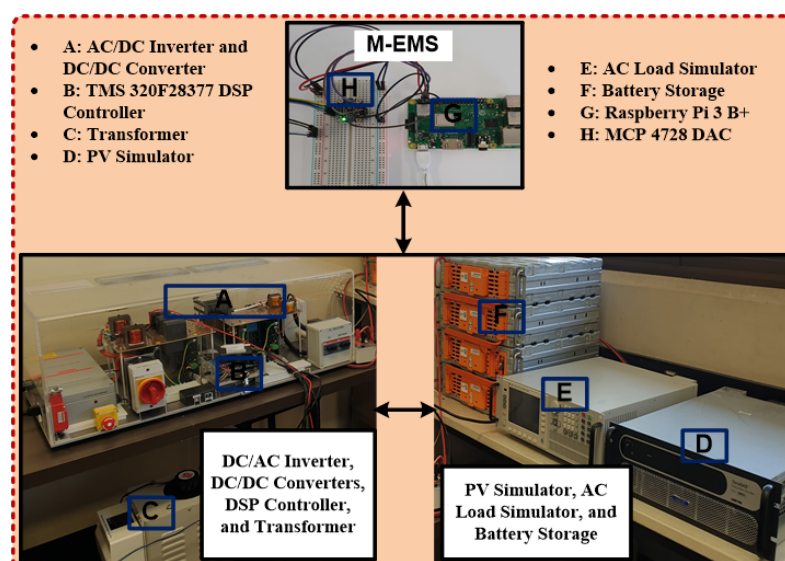

Figure 5. Experimental setup.

The experimental results comprises two sections, namely, forecasting and scheduling results. Firstly, the forecasting results are discussed. The forecasting is performed by using the proposed ensemble forecasting strategy and it involves the forecasting of PV power and load demand. The normalized root mean square error (NRMSE), mean absolute error (MAE), and absolute error (AE), are adopted to measure the forecasting accuracy of the proposed strategy. The NRMSE, MAE, and AE can be calculated as follows:

$$\text{NRMSE} = \frac{\sqrt{\frac{1}{N} \sum_{i=1}^{N} (A_t - P_t)}}{A_{t-max} - A_{t-min}} \tag{35}$$

$$\text{MAE} = \frac{1}{N} \sum_{i=1}^{N} | A_t - P_t | \tag{36}$$

$$\text{AE} = | A_t - P_t | \tag{37}$$

where P_t and A_t are forecasted and actual data, respectively, while N is the total number of samples. The hourly data of PV power, load demand, and correlated parameters from January 2016 to December 2017 are applied to study the performance of the proposed forecasting strategy. The PV power and load demand data set are taken from a residential home of Brisbane, and were provided by one of the Queensland energy providers, while the historical weather (temperature, wind speed, and humidity) data is taken from Griffith University weather station, Queensland. The hourly data samples of 2016 are applied for training, while the hourly data samples of 2017 are employed for validation and testing. The results for the proposed forecasting strategy are compared with ensemble strategy-1, PSO-ANN, and BPNN. The ensemble strategy-1 used similar forecasting models as the proposed strategy. However, the output of all models is aggregated using the equal weight combination method in ensemble strategy-1.

Figures 6–9 show the 24-h-ahead forecasting results of PV power and load demand for the chosen day of the case study. On the x-axis of each diagram, the time is depicted in hours, and on the y-axis of each diagram the power is depicted in watts (W). In experimental results, the data needs to be downscaled in order to display on the oscilloscope, therefore one hour is downscaled to 208 millisecond on the x-axis while the 500 W is downscaled to the 1 volt on the y-axis. The PV power forecasting result using the proposed ensemble strategy, ensemble strategy-1, PSO-ANN, and BPNN is depicted in Figures 6 and 7, while the AE values for all forecasting strategies are shown in Figure 10. It can be seen from Figures 6 and 7 that the proposed ensemble strategy has closer results in comparison with the other three strategies. The MAE and NRMSE values for the proposed strategy (43.4362 W and 1.3201%) are smaller than ensemble strategy-1 (68.9142 W and 2.0192%), PSO-ANN (93.4732 W, 2.7654%), and BPNN (133.5195 W, 5.0825%). A similar kind of trend is observed for the maximum AE value of all strategies. However, the minimum AE value for BPNN is lower than for the other three strategies.
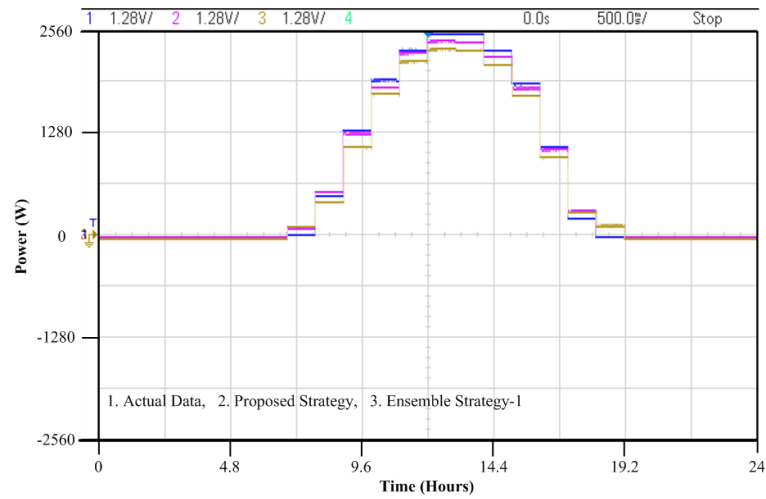
Figure 6. Forecasting result of PV power with proposed ensemble strategy and ensemble strategy-1.
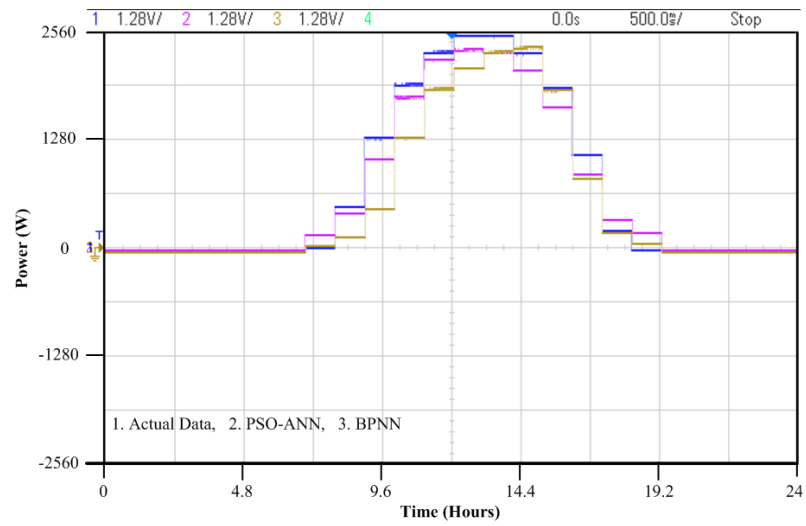

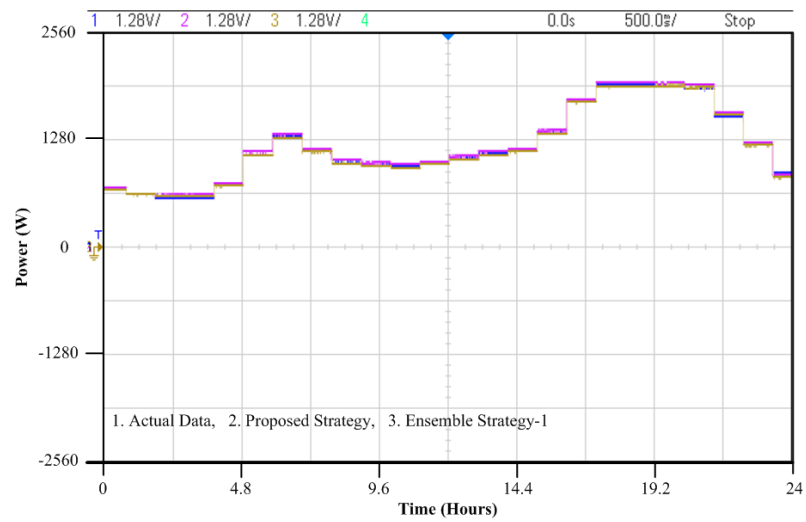**Figure 7.** Forecasting result of PV power with PSO-ANN and BPNN.

Figure 8. Forecasting result of load demand with proposed ensemble strategy and ensemble strategy-1.
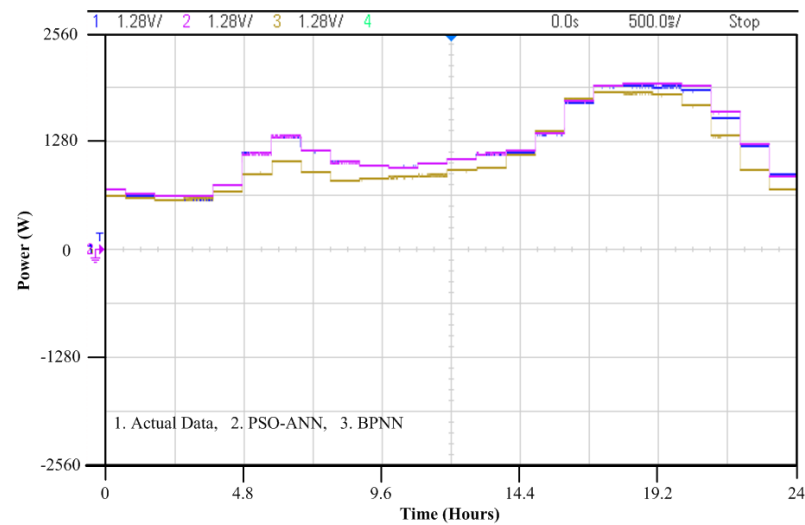
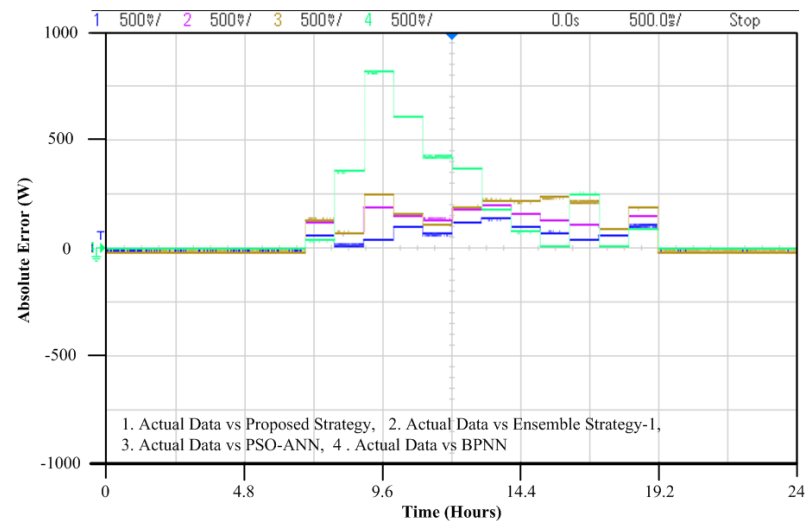**Figure 9.** Forecasting result of load demand with PSO-ANN and BPNN.

Figure 10. Absolute error of all strategies for PV power forecasting.

Figures 8 and 9 show the forecasting results of load demand with the proposed strategy, ensemble strategy-1, PSO-ANN, and BPNN, while Figure 11 illustrated the values of AE of all forecasting strategies for load demand forecasting. It is clearly shown from the graphs that the proposed ensemble strategy forecasts the load demand more accurately compared to other strategies. The proposed strategy (0.3848%) has a lower NRMSE value in contrast with ensemble strategy-1 (0.5347%), PSO-ANN (0.6550%), and BPNN (3.8287%). Similarly, the efficiency trend in terms of MAE, maximum and minimum AE values for all strategies have been seen. It can be seen from forecasting results that the proposed ensemble strategy, ensemble strategy-1, and PSO-ANN provided better accuracy than BPNN. Because the IPSO and PSO provided the optimized weights and biases of FNN/ANN which improved the forecasting accuracy significantly. Moreover, the IPSO and PSO did not trap in local minima like the backpropagation (BP) algorithm.
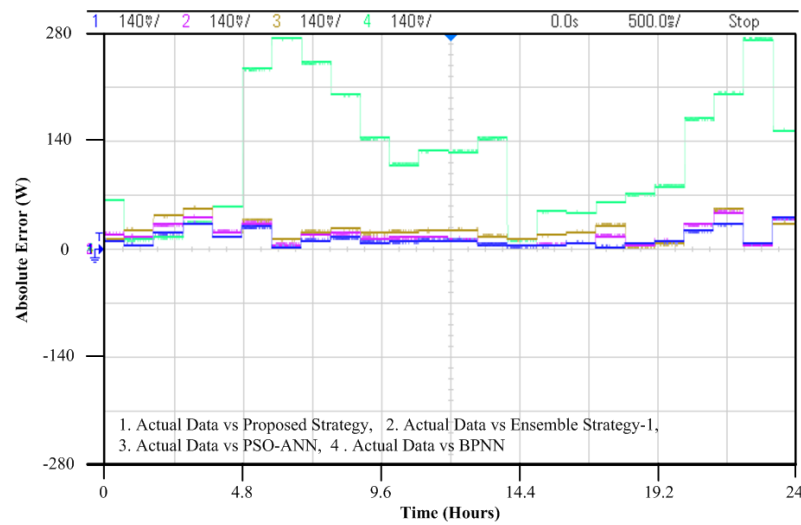
Figure 11. Absolute error of all strategies for load demand forecasting.

In this research, a 7000 W PV and 10,000 Wh Li-ion battery energy storage system (BESS) based grid-connected residential MG is studied as a case study to feed the residential load demand. Three different scenarios, i.e., P_{BC} is equal to P_{BD}, P_{BC} is greater than P_{BD}, and P_{BC} is less than P_{BD}, have been considered for analyzing the performance of GWO based scheduling. Moreover, the deb rule is used to handle the system constraints in GWO based scheduling. The maximum and minimum limits for imported and exported power from the main grid for all scenarios are 0 and 2500 W, respectively. Similarly, the PV power and load demand have the same values for all scenarios and are shown in Figure 12. The maximum, minimum, and initial capacity of BESS are the same for the three scenarios of 9000 Wh, 1000 Wh, and 4500 Wh. However, the maximum and minimum limits of discharge and charge power of BESS is different and given in Table 1.
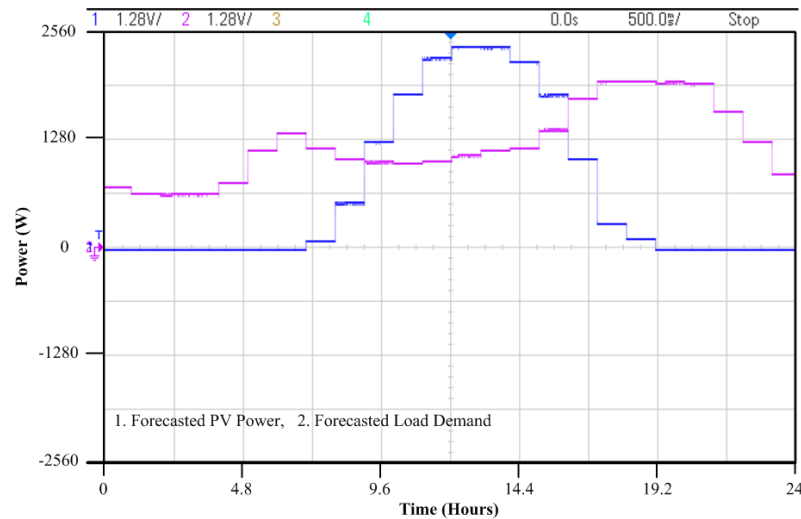

Figure 12. Forecasted PV power and load demand.

Table 1. Discharging and charging power limit of BESS.

Scenario	Parameter of BESS	Minimum Limit	Maximum Limit
Scenario-1	Discharging Power	0	1000 W
	Charging Power	0	1000 W
Scenario-2	Discharging Power	0	500 W
	Charging Power	0	1000 W
Scenario-3	Discharging Power	0	1000 W
	Charging Power	0	500 W

The efficiency of BESS is taken as 95%. The operational and maintenance cost of PV is negligible in Australia, but BESS has 0.001 cents per Wh operational and maintenance cost. The residential grid tariff is dependent on time, i.e., off-peak, shoulder peak, and peak hours in Australia, and it is known as the time of use tariffs (ToU) which is decided by the Australian Government, and is taken from the "made energy easy" website which was accessed in 2020. During the off-peak hours (10 p.m.–7 a.m.), the electricity buying price is 0.0205 cents per Wh; during shoulder peak hours (7 a.m.–4 p.m., 8 p.m.–10 p.m.) it is 0.0255 cents per Wh; and during peak hours (4 p.m.–8 p.m.), it is 0.0345 cents per Wh. The price of power selling to the grid is 0.0095 cents per Wh.

Figures 13–18 depict the experimental results of grid power and BESS power, while the capacity of BESS for day-ahead is shown in Figure 19. In all three scenarios, the cost of residential MG is minimized through the proper utilization of BESS. The grid power includes the imported and exported power from the main grid, while the BESS power comprises the discharging and charging power of the BESS. It can be seen from the results that the value of imported power from the grid for three scenarios is 22,112.43 W, 22,420.64 W, and 21,104.57 W, respectively, while the exported power to the grid is 3155.843 W, 3464.367 W, and 2148.809 W. Similarly, the values of discharging for BESS for all scenarios are 7742.885 W, 7415.042 W, and 5265.454 W. However, the charging power of BESS in the study scenarios is 7743.319 W, 7415.161 W, and 5265.057 W.
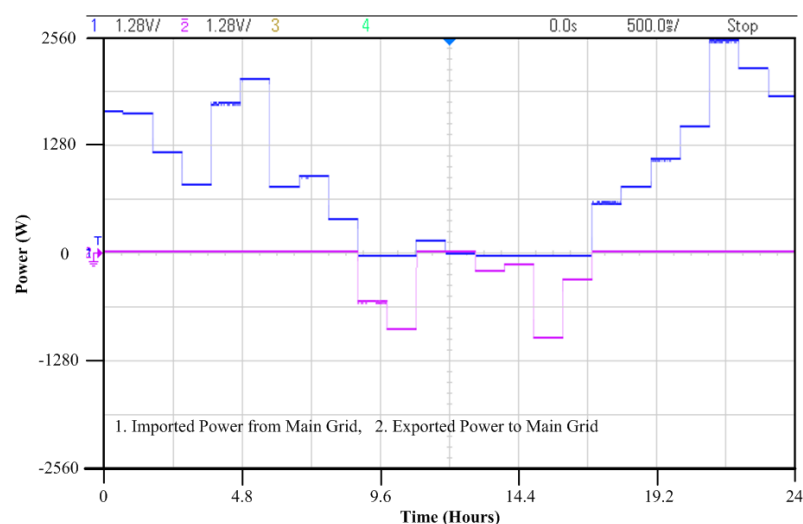
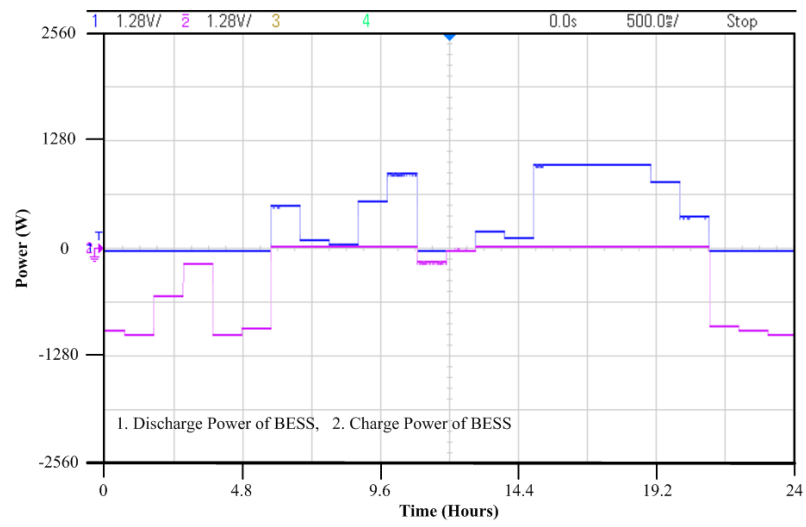**Figure 13.** Grid power for scenario-1.
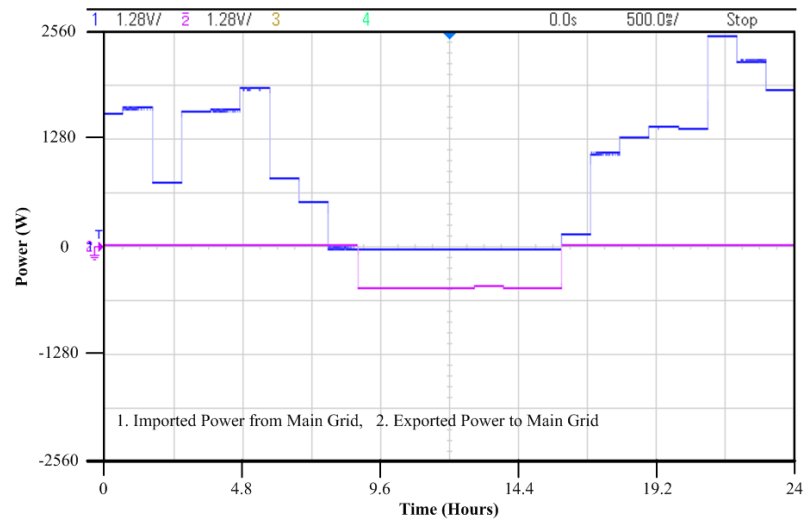
Figure 14. BESS power for scenario-1.
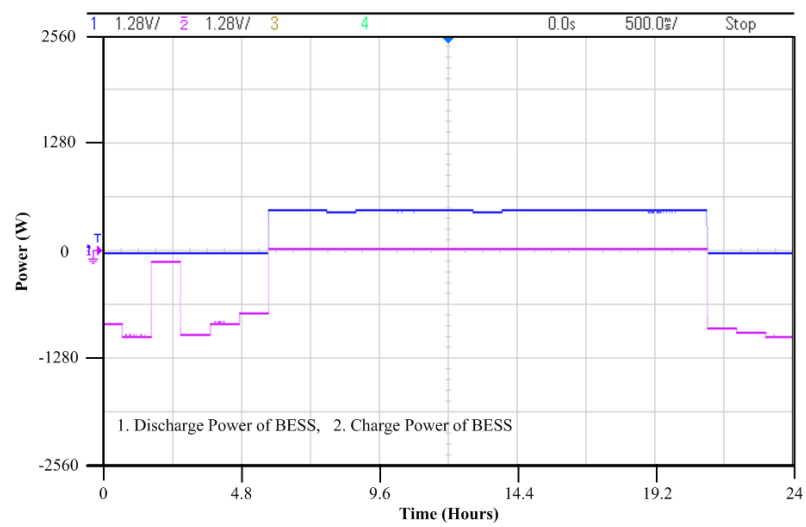

Figure 15. Grid power for scenario-2.

Figure 16. BESS power for scenario-2.

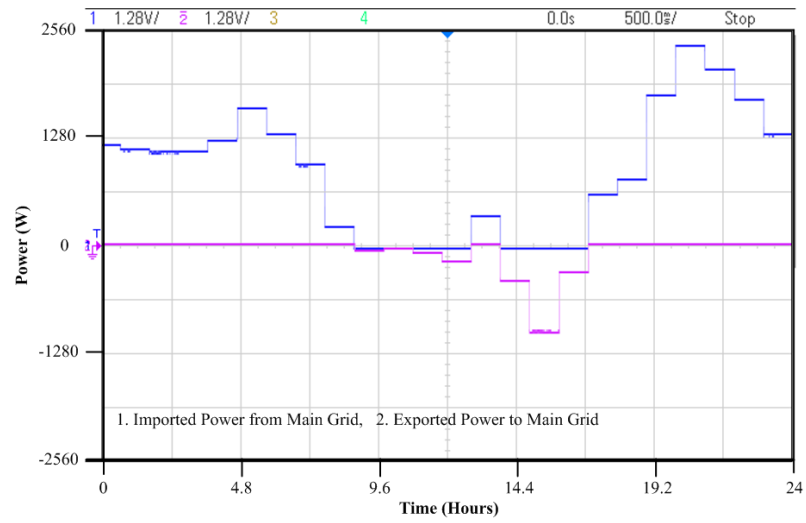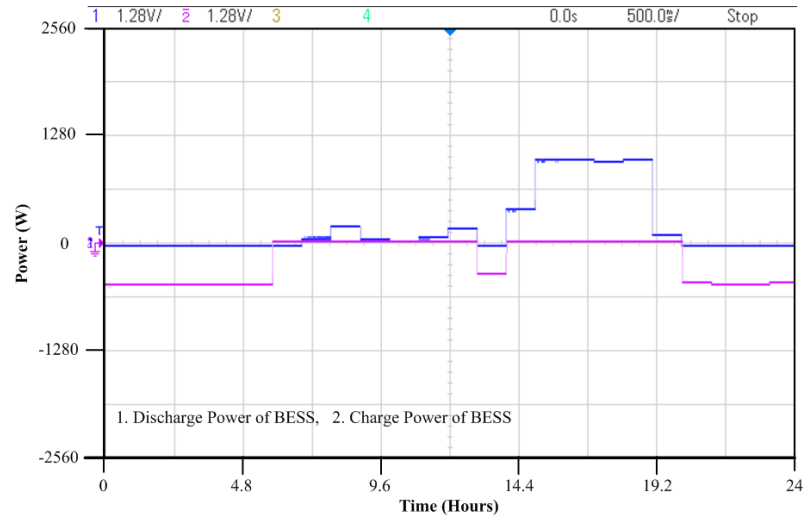**Figure 17.** Grid power for scenario-3.
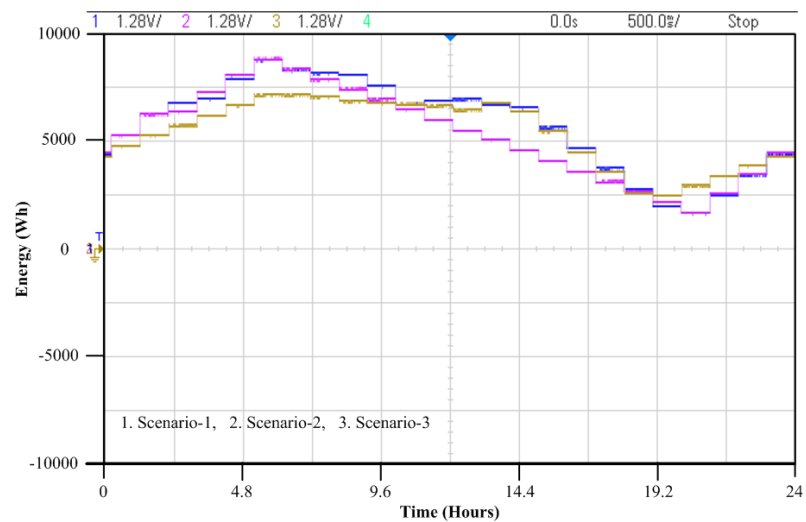

Figure 18. BESS power for scenario-3.

Figure 19. BESS capacity for all scenarios.

The overall optimum operating cost for all scenarios using GWO based scheduling is 483.62 cents, 499.09 cents, and 478.22 cents for the whole day. Scenario-3 provides

the minimum cost among all the scenarios because the BESS takes the lowest power for charging during shoulder peak compared to the other scenarios, which can be seen from Figure 19. However, the BESS took the highest power for charging during shoulder peak in other two scenarios, which increased the overall operating cost of residential MG.

5. Conclusions

In this paper, an M-EMS has been proposed to perform the day-ahead forecasting of PV power and load demand, and minimize the operational cost of grid-tied residential MG. The proposed M-EMS consisted of four different modules, i.e., forecasting, scheduling, data acquisition (DAQ), and human–machine interface (HMI) modules. An improved ensemble forecasting strategy that is a combination of three feedforward neural network models which are trained by using improved PSO was proposed in the forecasting module of M-EMS for day-ahead prediction of PV power and load demand. The grey wolf optimization-based scheduling strategy was proposed in the scheduling module of M-EMS to perform the optimum power flow of grid-connected residential MG. The DAQ and HMI module was utilized to monitor, analyze, and modify the input parameters of the forecasting and scheduling module. Finally, the proposed forecasting and scheduling strategy of M-EMS was implemented using Raspberry Pi 3 B+ and validated through a small-scale experiment. The experimental results indicate that the proposed forecasting strategy (1.3201% and 0.3848%) of M-EMS provides lower values of NRMSE as compared to ensemble strategy-1 (2.0192% and 0.5347%), PSO-ANN (2.7654% and 0.6550%), and BPNN (5.0825% and 3.8287%) for forecasting of PV power and load demand. Similarly, the results of the scheduling module of M-EMS show that scenario-3 provides minimum overall operational cost of grid-connected residential MG among all the scenarios. The forecasting accuracy of the improved ensemble forecasting strategy of the proposed M-EMS had limitations due to the selection of a single optimization algorithm for optimizing the weights and biases of FNN with different numbers of hidden layers. In addition, the deb rule was used as a constraint handling method in the GWO based scheduling strategy of the proposed M-EMS, which could provide premature convergence and lead to poor scheduling strategy performance due to the existing overpressure on feasibility region. In future work, the proposed M-EMS of grid-connected residential MG can be improved by integrating with it, a better forecasting strategy and/or scheduling strategy. Another possible extension in the proposed M-EMS might be to consider the battery degradation cost and/or emission cost.

Author Contributions: Conceptualization, U.B.T. and J.L.; Methodology, U.B.T., J.L. and S.T.; Validation, U.B.T., J.L. and S.T.; Investigation and Analysis, U.B.T., J.L. and S.T.; Writing—Original Draft Preparation, U.B.T.; Writing—Review and Editing, U.B.T., J.L., S.T., A.S.M.M. and M.K.; Supervision and Project Administration, J.L. All authors have read and agreed to the published version of the manuscript.

Abbreviations

AE	Absolute error
ANN	Artifical neural network
BESS	Battery energy storage system
BMA	Bayesian model averaging
BPNN	Backpropagation neural netwok
DE	Differential evolution
GA	Genetic algorithm
GWO	Grey wolf optimization
FNN	Feedforward neural network
LP	Linear programming
MG	Microgrid
MAE	Means absolute error
M-EMS	Microgrid energy management system
MILP	Mixed integer linear programming
NRMSE	Normalized root means square error
PSO	Particle swarm optimization
PV	Photovoltaic

References

1. Meng, L.; Sanseverino, E.R.; Luna, A.; Dragicevic, T.; Vasquez, J.C.; Guerrero, J.M. Microgrid supervisory controllers and energy management systems: A literature review. *Renew. Sustain. Energy Rev.* **2016**, *60*, 1263–1273. [CrossRef]
2. Guerrero, J.M.; Vasquez, J.C.; Matas, J.; Vicuna, L.G.; Castilla, M. Hierarchical Control of Droop-Controlled AC and DC Microgrids—A General Approach Toward Standardization. *IEEE Trans. Ind. Electron.* **2011**, *58*, 158–172. [CrossRef]
3. Katiraei, F.; Iravani, R.; Hatziargyriou, N.; Dimeas, A. Microgrids management. *IEEE Power Energy Mag.* **2008**, *6*, 54–65. [CrossRef]
4. Ziogou, C.; Ipsakis, D.; Seferlis, P.; Bezergianni, S.; Papadopoulou, S.; Voutetakis, S. Optimal production of renewable hydrogen based on an efficient energy management strategy. *Energy* **2013**, *55*, 58–67. [CrossRef]
5. Rafique, S.F.; Jianhua, Z. Energy management system, generation and demand predictors: A review. *IET Gener. Transm. Distrib.* **2018**, *12*, 519–530. [CrossRef]
6. Almada, J.B.; Leão, R.P.S.; Sampaio, R.F.; Barroso, G.C. A centralized and heuristic approach for energy management of an AC microgrid. *Renew. Sustain. Energy Rev.* **2016**, *60*, 1396–1404. [CrossRef]
7. Kanchev, H.; Lu, D.; Colas, F.; Lazarov, V.; Francois, B. Energy management and operational planning of a microgrid with a pv-based active generator for smart grid applications. *IEEE Trans. Ind. Electron.* **2011**, *58*, 4583–4592. [CrossRef]
8. Fossati, J.P.; Galarza, A.; Martín, V.A.; Echeverría, J.M.; Fontán, L. Optimal scheduling of a microgrid with a fuzzy logic controlled storage system. *Int. J. Electr. Power Energy Syst.* **2015**, *68*, 61–70. [CrossRef]
9. Santis, E.D.; Rizzi, A.; Sadeghian, A. Hierarchical genetic optimization of a fuzzy logic system for energy flows management in microgrids. *Appl. Soft Comput.* **2017**, *60*, 135–149. [CrossRef]
10. Sukumar, S.; Mokhlis, H.; Mekhilef, S.; Naidu, K.; Karimi, M. Mix-mode energy management strategy and battery sizing for economic operation of grid-tied microgrid. *Energy* **2017**, *118*, 1322–1333. [CrossRef]
11. Igualada, L.; Corchero, C.; Zambrano, M.C.; Heredia, F. Optimal energy management for a residential microgrid including a vehicle-to-grid system. *IEEE Trans. Smart Grid* **2014**, *5*, 2163–2172. [CrossRef]
12. Shen, J.; Jiang, C.; Liu, Y.; Qian, J. A microgrid energy management system with demand response for providing grid peak shaving. *Electr. Power Compon. Syst.* **2016**, *44*, 843–852. [CrossRef]
13. Tenfen, D.; Finardi, E.C. A mixed integer linear programming model for the energy management problem of microgrids. *Electr. Power Syst. Res.* **2015**, *122*, 19–28. [CrossRef]
14. Li, H.; Eseye, A.T.; Zhang, J.; Zheng, D. Optimal energy management for industrial microgrids with high-penetration renewables. *Prot. Control. Mod. Power Syst.* **2017**, *2*, 1–14. [CrossRef]
15. Eseye, A.T.; Zheng, D.; Li, H.; Zhang, J. Grid-price dependent optimal energy storage management strategy for grid-connected industrial microgrids. In Proceedings of the 2017 Ninth Annual IEEE Green Technologies Conference (GreenTech), Denver, CO, USA, 29–31 March 2017.
16. Faridnia, N.; Habibi, D.; Lachowicz, S.; Kavousifard, A. Optimal scheduling in a microgrid with a tidal generation. *Energy* **2019**, *171*, 435–443. [CrossRef]
17. Alavi, S.A.; Ahmadian, A.; Aliakbar,G.M. Optimal probabilistic energy management in a typical micro-grid based-on robust optimization and point estimate method. *Energy Convers. Manag.* **2015**, *95*, 314–325. [CrossRef]
18. Mohan, V.; Singh, J.G.; Ongsakul, W. An efficient two stage stochastic optimal energy and reserve management in a microgrid. *Appl. Energy* **2015**, *160*, 28–38. [CrossRef]

19. Sedighizadeh, M.; Esmaili, M.; Jamshidi, A.; Ghaderi, M.H. Stochastic multi-objective economic-environmental energy and reserve scheduling of microgrids considering battery energy storage system. *Int. J. Electr. Power Energy Syst.* **2019**, *106*, 1–16. [CrossRef]
20. Radosavljević, J.; Jevtić, M.; Klimenta, D. Energy and operation management of a microgrid using particle swarm optimization. *Eng. Optim.* **2016**, *48*, 811–830. [CrossRef]
21. García-Triviño, P.; Llorens-Iborra, F.; García-Vázquez, C.A.; Gil-Mena, A.J.; Fernández-Ramírez, L.M.; Jurado, F. Long-term optimization based on PSO of a grid-connected renewable energy/battery/hydrogen hybrid system. *Int. J. Hydrogen Energy* **2014**, *39*, 10805–10816. [CrossRef]
22. Hossain, M.A.; Pota, H.R.; Squartini, S.; Zaman, F.; Guerrero, J.M. Energy scheduling of community microgrid with battery cost using particle swarm optimisation. Applied Energy. *Appl. Energy* **2019**, *254*, 113723. [CrossRef]
23. Hossain, M.A.; Chakrabortty, R.K.; Ryan, M.J.; Pota, H.R. Energy management of community energy storage in grid-connected microgrid under uncertain real-time prices. *Sustain. Cities Soc.* **2021**, *66*, 102658. [CrossRef]
24. Golshannavaz, S.; Afsharnia, S.; Siano, P. A comprehensive stochastic energy management system in reconfigurable microgrids. *Int. J. Energy Res.* **2016**, *40*, 1518–1531. [CrossRef]
25. Nemati, M.; Braun, M.; Tenbohlen, S. Optimization of unit commitment and economic dispatch in microgrids based on genetic algorithm and mixed integer linear programming. *Appl. Energy* **2018**, *210*, 944–963. [CrossRef]
26. Tayab, U.B.; Zia, A.; Yang, F.; Lu, J.; Kashif, M. Short-term load forecasting for microgrid energy management system using hybrid HHO-FNN model with best-basis stationary wavelet packet transform. *Energy* **2020**, *203*, 117857. [CrossRef]
27. Hassan, S.; Khosravi, A.; Jaafar, J. Examining performance of aggregation algorithms for neural network-based electricity demand forecasting. *Int. J. Electr. Power Energy Syst.* **2015**, *64*, 1098–1105. [CrossRef]
28. Eseye, A.T.; Zhang, J.; Zheng, D. Short-term photovoltaic solar power forecasting using a hybrid Wavelet-PSO-SVM model based on SCADA and Meteorological information. *Renew. Energy* **2018**, *118*, 357–367. [CrossRef]
29. Shao, B.; Li, M.; Zhao, Y.; Bian, G. Nickel Price Forecast Based on the LSTM Neural Network Optimized by the Improved PSO Algorithm. *Math. Probl. Eng.* **2019**, *2019*, 1934796. [CrossRef]
30. Mirjalili, S.; Mirjalili, S.M.; Lewis, A. Grey Wolf Optimizer. *Adv. Eng. Softw.* **2014**, *69*, 46–61. [CrossRef]